

**Quasi-exact solution to the Dirac equation for the hyperbolic-secant potential**

R. R. Hartmann\*

*Physics Department, De La Salle University, 2401 Taft Avenue, Manila, Philippines*

M. E. Portnoi†

*School of Physics, University of Exeter, Stocker Road, Exeter EX4 4QL, United Kingdom  
and International Institute of Physics, Av. Odilon Gomes de Lima, 1722, Capim Macio, CEP 59078-400, Natal RN, Brazil  
(Received 20 May 2013; revised manuscript received 7 November 2013; published 2 January 2014)*

We analyze bound modes of two-dimensional massless Dirac fermions confined within a hyperbolic secant potential, which provides a good fit for potential profiles of existing top-gated graphene structures. We show that bound states of both positive and negative energies exist in the energy spectrum and that there is a threshold value of the characteristic potential strength for which the first mode appears. Analytical solutions are presented in several limited cases and supercriticality is discussed.

DOI: [10.1103/PhysRevA.89.012101](https://doi.org/10.1103/PhysRevA.89.012101)

PACS number(s): 03.65.Pm, 81.05.ue, 03.65.Ge

**I. INTRODUCTION**

Transmission resonances and supercriticality [1] (bound states occurring at  $E = -m$ , where  $E$  is the particles energy and  $m$  the particles mass) of relativistic particles in one-dimensional potential wells have been studied extensively [1–10]. Analytic solutions have been obtained for the square well [2,3], Woods-Saxon potential [4], cusp potential [5], and Hulthén potential [6] as well as asymmetric barriers [7,8], multiple barriers [9], and a class of short-range potentials [10]. The successful isolation of graphene [11] has led to renewed interest in the transmission-reflection problem for the one-dimensional Dirac equation.

The carriers within graphene, a single layer of carbon atoms in a honeycomb lattice, behave as two-dimensional massless Dirac fermions [12]. In the presence of an electric field, their massless relativistic nature results in drastically different behavior to their normal nonrelativistic electron counterparts; for example, backscattering is forbidden for carriers which are incident normal to the barrier [13–15]. However, they can be reflected at non-normal incidence, and therefore confinement is possible.

Electron wave guides in graphene have been studied extensively both theoretically and experimentally. It has been shown that it is possible to confine graphene electrons by electrostatic potentials [16–28], magnetic barriers [29–39], and strain-induced fields [40–43]. Transmission through symmetric [15–18,27,28,32,44–56] and asymmetric electrostatic barriers [25] have been studied and fully confined modes within a smooth one-dimensional potential have been predicted to exist at zero energy [57,58]. The majority of electrostatically defined wave guides have been limited to sharp barriers (i.e., potentials which are noncontinuous). However, unlike in semiconductor heterostructures or dielectric waveguides for light, finite square wells and other sharply terminated finite barriers have not yet been experimentally demonstrated in graphene, as potential profiles are created by electrostatic gating, which results in smooth potentials [49–55].

The conduction and valence bands in graphene touch each other at six points, which lie on the edge of the first Brillouin zone. In pristine undoped graphene the Fermi surface coincides with these points (known as Dirac points), and at these points the dispersion relation is linear [59]. Two of these points are inequivalent and degenerate in terms of energy. A sharp barrier results in intervalley scattering; therefore the full treatment of a sharp boundary requires the mixing of two Dirac cones. Therefore to stay within a single cone approximation many authors introduce the term “smooth steplike potential,” since smooth potentials changing slowly on the spatial scale exceeding tens of graphene lattice constants, like the one considered in this paper, do not result in intervalley scattering. Furthermore, for sharp barriers, the discontinuity of the potential results in discontinuities in the wave function’s derivative which have to be treated with special care [60]; this is not the case for smooth potentials.

Exact solutions of the one-dimensional Dirac equation are not only useful in the analytic modeling of physical systems, but they are also important for testing numerical, perturbative, or semiclassical methods [28]. The hyperbolic secant potential belongs to the class of quantum models which are quasi-exactly solvable [61–64], where only some of the eigenfunctions and eigenvalues are found explicitly.

In this paper we obtain the bound state energies contained within the hyperbolic secant potential in pristine graphene and supercriticality is discussed. Hitherto unknown analytical solutions for certain bound modes contained within this model potential are presented. We show that bound states of both positive and negative energies exist in the spectrum and that there is a threshold value of the characteristic potential strength for which the first mode appears, in striking contrast to the nonrelativistic case.

**II. BOUND MODES IN A MODEL POTENTIAL**

The Hamiltonian operator in the massless Dirac-Weyl model for graphene, which describes the motion of a single electron in the presence of a one-dimensional potential  $U(x)$ , is

$$\hat{H} = v_F(\sigma_x \hat{p}_x + \sigma_y \hat{p}_y) + U(x), \quad (1)$$

\*richard.hartmann@dlsu.edu.ph

†m.e.portnoi@exeter.ac.uk

where  $\sigma_{x,y}$  are the Pauli spin matrices,  $\hat{p}_x = -i\hbar\frac{\partial}{\partial x}$  and  $\hat{p}_y = -i\hbar\frac{\partial}{\partial y}$  are the momentum operators in the  $x$  and  $y$  directions, respectively, and  $v_F \approx 10^6$  m/s is the Fermi velocity in graphene. In what follows we will consider a smooth confining potential, the hyperbolic secant potential, which does not mix the two nonequivalent valleys. All our results herein can be easily reproduced for the other valley. When Eq. (1) is applied to a two-component Dirac wave function of the form

$$e^{ik_y y} \begin{pmatrix} \Psi_A(x) \\ \Psi_B(x) \end{pmatrix},$$

where  $\Psi_A(x)$  and  $\Psi_B(x)$  are the wave functions associated with the  $A$  and  $B$  sublattices of graphene, respectively, and the free motion in the  $y$  direction is characterized by the wave vector  $k_y$  measured with respect to the Dirac point, the following coupled first-order differential equations are obtained:

$$[V(x) - \varepsilon]\Psi_A - i\left(\frac{d}{dx} + k_y\right)\Psi_B = 0 \quad (2)$$

and

$$[V(x) - \varepsilon]\Psi_B - i\left(\frac{d}{dx} - k_y\right)\Psi_A = 0. \quad (3)$$

Here  $V(x) = U(x)/\hbar v_F$ , and energy,  $\varepsilon$ , is measured in units of  $\hbar v_F$ . For convenience let  $\Psi_A = (\Psi_1 + \Psi_2)/2$  and  $\Psi_B = (\Psi_1 - \Psi_2)/2$ ; therefore Eqs. (2)–(3) become

$$\left[V(x) - \varepsilon - i\frac{d}{dx}\right]\Psi_1 + ik_y\Psi_2 = 0 \quad (4)$$

and

$$\left[V(x) - \varepsilon + i\frac{d}{dx}\right]\Psi_2 - ik_y\Psi_1 = 0. \quad (5)$$

Equations (4)–(5) can then be reduced to a single second-order differential equation in  $\Psi_1$  ( $\Psi_2$ ):

$$\left\{[V(x) - \varepsilon]^2 - k_y^2 \pm i\frac{dV(x)}{dx}\right\}\Psi_{1,2} + \frac{d^2\Psi_{1,2}}{dx^2} = 0. \quad (6)$$

The plus and minus signs correspond to wave function  $\Psi_1$  and  $\Psi_2$ , respectively. The potential under consideration is defined as

$$V(x) = -\frac{V_0}{\cosh(x/l)}, \quad (7)$$

where  $V_0$  and  $l$  characterize the potential strength and width, respectively. This potential is known to admit analytic solutions for the case of  $\varepsilon = 0$  [57,65] and is a good representation of experimentally generated potential profiles [50–55]. For top-gated structures, the width of the potential is defined by the geometry of the top gate structure, and the strength of the potential is defined by the voltage applied to the top gate.

It should be noted that many unusual situations may arise in one-dimensional quantum mechanics due to the presence of a delta function when the usual definition does not hold true. In certain instances, the one-dimensional Dirac equation, which has a wave function defined by a differential equation involving the delta function, can result in the usual definition of the delta function being inconsistent with the definition of the wave function itself [66–68]. The implications of such

situations regarding the transmission-reflection problem in one-dimensional quantum mechanics are reviewed at length in Ref. [69]. In the limit that  $l \rightarrow 0$  the hyperbolic secant potential smoothly approaches a  $\delta$ -function potential, thus making it an ideal approximation.

Let us search for solutions of Eq. (6) with the potential given by Eq. (7) in the form

$$\Psi_{1,2} = A_{1,2} V^\kappa \psi_{1,2}(x), \quad (8)$$

where

$$\kappa = l\sqrt{k_y^2 - \varepsilon^2} \quad (9)$$

and  $A_{1,2}$  is a constant. Substitution of Eq. (8) into Eq. (6) yields

$$\begin{aligned} & \frac{d^2\psi_{1,2}}{dz^2} - 8\kappa \frac{\tanh(z)}{1 + \tanh^2(z)} \frac{d\psi_{1,2}}{dz} \\ & + 4 \left\{ 2w \left[ S_E \sqrt{\Delta^2 - \kappa^2} + S_\Psi \frac{\tanh(z)}{1 + \tanh^2(z)} i \right] \frac{1 - \tanh^2(z)}{1 + \tanh^2(z)} \right. \\ & \left. + [w^2 - \kappa(\kappa + 1)] \left[ \frac{1 - \tanh^2(z)}{1 + \tanh^2(z)} \right]^2 \right\} \psi_{1,2} = 0, \quad (10) \end{aligned}$$

where we use the dimensionless variables  $w = V_0 l$ ,  $\Delta = k_y l$ ,  $E = \varepsilon l$ , and  $z = x/2l$ .  $S_E = 1$  for  $E > 0$  and  $S_E = -1$  for  $E < 0$ .  $S_\Psi = 1$  for  $\Psi_1$  and  $S_\Psi = -1$  for  $\Psi_2$ . Using the transformation  $\psi_{1,2} = (\xi - \frac{1}{2})^\mu H_{1,2}(\xi)$  with the change of variable

$$\xi = \frac{e^{-i\frac{\pi}{4}} \tanh(z) + 1}{\sqrt{2} \tanh(z) - i},$$

where

$$\mu = \kappa + S_\mu w + \frac{1}{2}(1 + S_\mu S_\Psi) \quad (11)$$

and  $S_\mu = \pm 1$ , allows Eq. (10) to be reduced to

$$\begin{aligned} & \frac{d^2 H_{1,2}}{d\xi^2} + \left[ \frac{\gamma}{\xi} + \frac{\delta}{\xi - 1} + \frac{\epsilon}{\xi - a} \right] \frac{dH_{1,2}}{d\xi} \\ & + \frac{\alpha\beta\xi - q}{\xi(\xi - 1)(\xi - a)} H_{1,2} = 0, \quad (12) \end{aligned}$$

where

$$\epsilon = \alpha + \beta - \gamma - \delta + \frac{1}{2},$$

$$\gamma = \delta = 1 + 2\kappa,$$

$$a = \frac{1}{2},$$

$$\beta = \frac{2}{\alpha} [S_\Psi w + (1 + 2\kappa)\mu],$$

$$2\alpha = 2\mu + 2\kappa + 1$$

$$\pm \sqrt{(2\mu + 2\kappa + 1)^2 - 8[S_\Psi w + (1 + 2\kappa)\mu]},$$

$$q = \frac{\alpha\beta}{2} + i2S_E w \sqrt{\Delta^2 - \kappa^2},$$

and  $H_{1,2}$  is the Heun function given by the expression [70]

$$H_{1,2} = H_{1,2}(a, q; \alpha, \beta, \gamma, \delta, \xi) = \sum_{j=0}^{\infty} c_j \xi^j, \quad (13)$$

where

$$c_0 = 1, \quad a\gamma c_1 - qc_0 = 0, \\ R_j c_{j+1} - (Q_j + q)c_j + P_j c_{j-1} = 0,$$

with

$$P_j = (j - 1 + \alpha)(j - 1 + \beta), \\ Q_j = j[(j - 1 + \gamma)(1 + a) + a\delta + \epsilon], \\ R_j = a(j + 1)(j + \gamma).$$

The bound-state energies are determined by the boundary condition  $\Psi_{1,2}(\pm\infty) = 0$ . For the case of  $x \rightarrow -\infty, \xi \rightarrow 0$  and the right-hand side of Eq. (13) equals unity; therefore, it can be seen from Eq. (8) that the boundary condition  $\Psi_{1,2}(-\infty) = 0$  requires  $\kappa$  to exceed zero. In the limit that  $x \rightarrow \infty, \xi \rightarrow 1$  the bound state solutions correspond to combinations of the accessory and exponent parameters, which result in nondivergent values of Eq. (13). In certain instances Eq. (13) can be reduced to a finite polynomial of degree  $n$  admitting analytic results. However, applying symmetry conditions to the wave function Eq. (8) is sufficient to obtain the energy eigenvalue spectrum.

It is clear from Eqs. (4)–(5) that neither  $\Psi_1$  nor  $\Psi_2$  are symmetrized wave functions, so we shall transform to the symmetrized functions:

$$\Psi_I = (\Psi_1 + \Psi_2) + i(\Psi_1 - \Psi_2), \\ \Psi_{II} = (\Psi_1 + \Psi_2) - i(\Psi_1 - \Psi_2). \tag{14}$$

When  $\Psi_I$  is an odd function  $\Psi_I(0) = 0$  and when  $\Psi_{II}$  is an even function  $\Psi_{II}(0) = 0$  these two boundary conditions result in the following transcendental equation:

$$2 \left[ (1 + S_\psi S_\mu)w + \frac{1}{2}(S_\psi + S_\mu) + E \mp \Delta \right] H_{1,2}(\xi_0) \\ + iS_\psi \left. \frac{dH_{1,2}(\xi)}{d\xi} \right|_{\xi=\xi_0} = 0, \tag{15}$$

where  $\xi_0 = e^{i\frac{\pi}{4}}/\sqrt{2}$  and the  $\mp$  sign corresponds to the odd (upper sign) and even (lower sign) bound modes. Equation (15) was solved numerically and the results are shown in Fig. 1 for the case of  $w = 3.2$ . The long-dashed lines represent  $\kappa = 0$ ; as  $\kappa \rightarrow 0, |E| \rightarrow |\Delta|$  and the bound states merge with the continuum, and the potential is said to be supercritical, where  $\Delta$  plays the role of mass. The zero transverse momentum wave functions (i.e.,  $\kappa = 0$ ) are half-bound; one component of the spinor wave function decays to zero at  $x = \pm\infty$ , and the other component decays to nonzero values. The half-bound states can be obtained from Eq. (15) with the substitution  $E = \pm\Delta$ . For the case of  $w = 3.2$ , the first half-bound state occurs at  $E = -1.232$ , and the corresponding wave function is plotted in Fig. 2. It should be noted that this wave function contains two additional stationary points in comparison to that of the square well [1]; however, they are indeed present for a Gaussian [1] and Woods-Saxon potential [4].

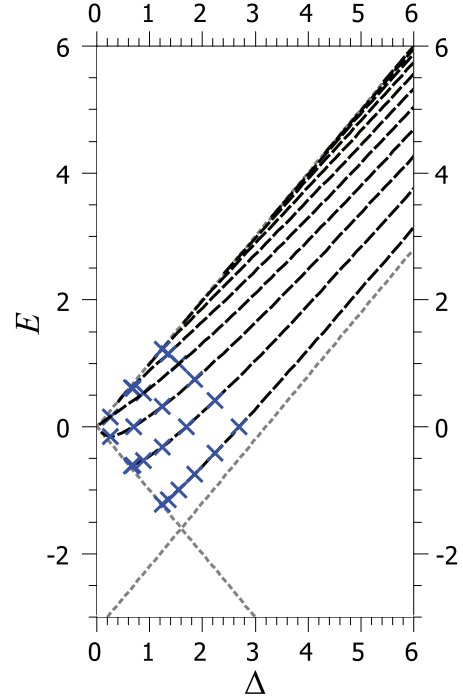


FIG. 1. (Color online) Energy spectrum of confined states in a hyperbolic-secant potential as a function of  $\Delta$  for  $w = 3.2$ . The black (long-dashed) lines represent the computational results, and the blue crosses the analytical results. The boundary at which the bound states merge with the continuum is denoted by the gray (short-dashed) lines.

### A. Exact solutions

In what follows we shall see that Eq. (15) can be solved exactly in a few limited cases. One condition that ensures  $\Psi_1$  is a nondivergent function at  $x \rightarrow \infty$  is that  $H_{1,2}$  is reduced to a finite polynomial. This occurs when two conditions are met:

$$\alpha = -n \tag{16}$$

and

$$q = q_{n,m}, \tag{17}$$

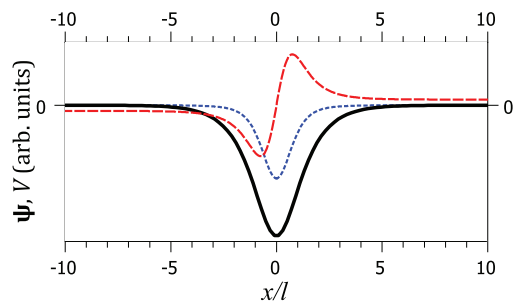


FIG. 2. (Color online) The lowest energy, zero transverse momentum wave function for the hyperbolic potential well (depicted by the black solid line) defined by  $w = 3.2$ . The real part of the wave functions  $\Psi_I$  and  $\Psi_{II}$  are shown in red (long-dashed) and blue (short-dashed), respectively.

where  $n$  and  $m$  are non-negative integers and  $m \leq n$ , and  $q_{n,m}$  are the eigenvalues of the tridiagonal matrix

$$\begin{bmatrix} 0 & a\gamma & 0 & \cdots & 0 \\ P_1 & -Q_1 & R_1 & \cdots & 0 \\ 0 & P_2 & -Q_2 & \cdots & 0 \\ \vdots & \vdots & \vdots & \ddots & R_{n-1} \\ 0 & 0 & 0 & P_n & -Q_n \end{bmatrix}.$$

In this instance,

$$H_1 = H(a, q_{n,m}; -n, \beta, \gamma, \delta, \xi) \quad (18)$$

is a polynomial of degree  $n$ , these solutions are the Heun polynomials, which have attracted a lot of recent attention in relation to various exactly solvable quantum mechanics problems (see Ref. [71] and references therein for a general review).

Since  $w$  and  $\kappa$  are positive quantities, in order to satisfy the termination condition, Eq. (16),  $S_\mu$  must take upon the value of  $-1$ ; therefore, Eq. (11) becomes

$$\mu = \kappa - w.$$

The first termination condition, Eq. (16), also requires

$$\kappa = w - \frac{n+1}{2}. \quad (19)$$

Therefore the exponent parameters become

$$\alpha = -n, \quad \beta = 2w - n - 1, \quad \gamma = \delta = 2w - n,$$

and the accessory parameter becomes

$$q_{n,m} = iS_E 2w \sqrt{\Delta^2 - \left(w - \frac{n+1}{2}\right)^2} - n \left(w - \frac{n+1}{2}\right). \quad (20)$$

When  $x \rightarrow -\infty$ ,  $\xi \rightarrow 0$ ; therefore, the right-hand side of Eq. (18) equals unity. The right-hand side of Eq. (18) can be expressed as  $H(1-a, -q_{nm} - \beta n; -n, \beta, \delta, \gamma; 1-\xi)$  [72]; therefore, as  $x \rightarrow \infty$ ,  $\xi \rightarrow 1$  and the Heun polynomial tends to unity; therefore, it can be seen from Eq. (8) that the boundary condition  $\Psi_{1,2}(\pm\infty) = 0$  requires  $\kappa$  to exceed zero, thus, we obtain the condition that  $w > \frac{(n+1)}{2}$ . It should be noted that this puts an upper limit on  $n$ , the order of termination of the Heun polynomial. From Eqs. (9) and (19) the exact Dirac energy spectrum is found to be

$$E_{n,m} = \pm \sqrt{\Delta_{n,m}^2 - \left(w - \frac{n+1}{2}\right)^2}, \quad (21)$$

where  $\Delta_{n,m}$  is a function of  $w$  and  $n$  and is found via the satisfaction of the second termination condition, Eq. (17). Let us first consider the case of  $E = 0$ ; in this instance the termination condition, Eq. (17), is satisfied when  $q_{n,m} = 0$ , which requires  $w = (n+1)/2$ , resulting in unbound states since in this instance  $\Delta_{n,m} = 0$ , or when

$$q_{n,m} = -n \left(w - \frac{n+1}{2}\right) = \frac{\alpha\beta}{2}, \quad (22)$$

which requires  $\Delta = \pm(w - \frac{n+1}{2})$ , and in this case the right-hand side of Eq. (18) becomes

$$H\left(\frac{1}{2}, \frac{\alpha\beta}{2}; \alpha, \beta, \gamma, \gamma, \xi\right). \quad (23)$$

Using the identity [72]  $H(a, q; \alpha, \beta, \gamma, \delta; z) = H(\frac{1}{a}, \frac{q}{a}; \alpha, \beta, \gamma, \alpha + \beta + 1 - \gamma - \delta; \frac{z}{a})$ , allows Eq. (23) to be reexpressed as

$$H(2, \alpha\beta; \alpha, \beta, \gamma, \alpha + \beta + 1 - 2\gamma; 2\xi),$$

which reduces to the Gauss hypergeometric function [73]

$${}_2F_1\left(\frac{1}{2}\alpha, \frac{1}{2}\beta; \gamma; 4\xi(1-\xi)\right).$$

In order to terminate the hypergeometric series and therefore obtain bound solutions it is necessary to satisfy the condition  $\alpha = -2N$ , where  $N$  is a positive integer; therefore,

$$\Delta = \pm\left(w - N + \frac{1}{2}\right),$$

where  $n = 2N$ , which restores the results obtained in Ref. [57]. It should be noted that the condition  $w > \frac{(n+1)}{2}$  puts an upper limit on  $n$ , the order of termination of the Heun polynomial. Notably the first mode occurs at  $n = 0$ , thus there is a lower threshold of  $w > \frac{1}{2}$  for which bound modes appear. Hence within graphene, quantum wells are very different to the nonrelativistic case; bound states are not present for any symmetric potential, they are present only for significantly strong or wide potentials, such that  $V_0l > \frac{1}{2}$ .

The nonzero exact energy eigenvalues are obtained by solving Eq. (20). When  $n = 0$  the eigenvalue is found to be  $E_{0,0} = 0$ , where  $\Delta_{0,0} = \pm(w - \frac{1}{2})$ . For the case of  $n = 1$ , which exists only when  $w$ , the characteristic potential strength, exceeds one, the eigenvalues are

$$E_{1,0} = -\frac{1}{2w} \sqrt{w^2 - w}$$

and

$$E_{1,1} = \frac{1}{2w} \sqrt{w^2 - w},$$

where

$$\Delta_{1,0} = \Delta_{1,1} = \pm \frac{2w-1}{2w} \sqrt{w^2 - w}.$$

Bound states of both positive and negative energies exist in the energy spectrum, which is markedly different to quantum wells in the nonrelativistic case. Each eigenvalue is twofold degenerate in terms of  $\Delta$ , the particles momentum along the barrier. In Fig. 3 we present  $\Psi_I$ ,  $\Psi_{II}$  and the corresponding electron density profiles for the  $E_{10}$  and  $E_{11}$  modes. It can be seen from Fig. 3 that upon changing the sign of  $\Delta$  the parity of  $\Psi_I$  and  $\Psi_{II}$  changes. This means backscattering within a channel requires a change in the parity of the wave functions and thus should be strongly suppressed. Such suppression should result in an increase in the mean free path of the channel compared to that of graphene. Each component of the spinor wave function acts much like the single component wave function of a conventional quantum well; when  $\Delta > 0$  ( $\Delta < 0$ ),  $\Psi_{II}$  ( $\Psi_I$ ) for the lowest energy state,  $E_{10}$ , is  $s$ -like

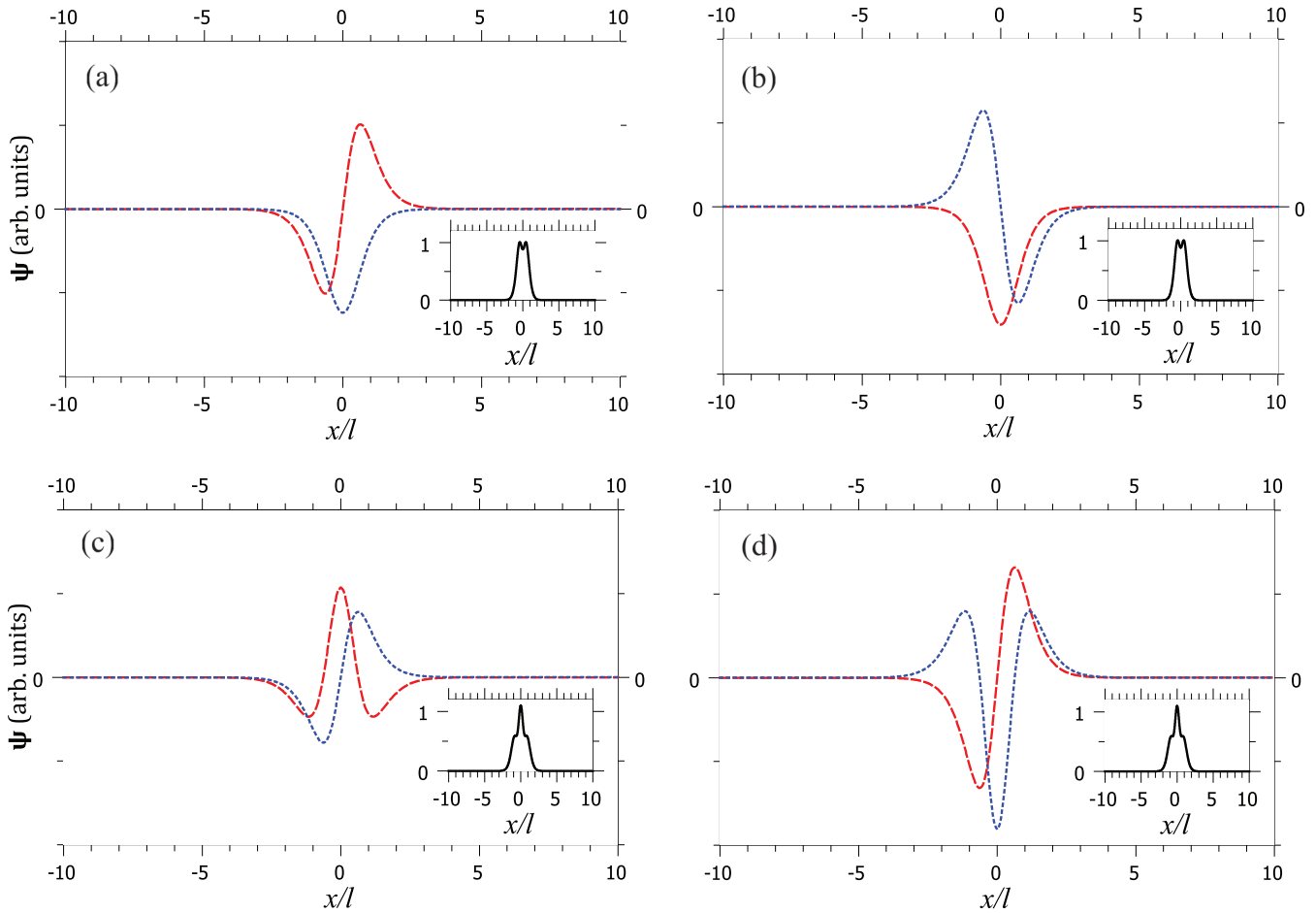


FIG. 3. (Color online) The real part of the wave functions  $\Psi_I$  (red long-dashed line) and  $\Psi_{II}$  (blue short-dashed line) are shown for  $\omega = 3.2$  for: (a) the  $E_{1,0}$  mode with  $\Delta > 0$ , (b) the  $E_{1,0}$  mode with  $\Delta < 0$ , (c) the  $E_{1,1}$  mode with  $\Delta > 0$ , and (d) the  $E_{1,1}$  mode with  $\Delta < 0$ . The insets show the electron density profile for the corresponding modes.

and for the next excited state,  $E_{11}$ ,  $p$ -like. Since  $\Psi_I$  ( $\Psi_{II}$ ) is the derivative of  $\Psi_{II}$  ( $\Psi_I$ ), it must be  $p$ -like for  $E_{10}$  and  $d$ -like for  $E_{11}$ . The  $E_{10}$  mode has a dip in the charge density profile at the middle of the potential well, whereas the  $E_{11}$  mode has a maximum. These counterintuitive density profiles arise from the complex two-component structure of the wave functions.

The bound modes which propagate along the potential well each contribute  $4e^2/h$  to the channels conductance, where the factor of four accounts for the valley and spin degeneracy. By modulating the parameters of the potential and or changing the position of the Fermi level one can increase the conductance of the channel by multiples of  $4e^2/h$ ; therefore a change of geometry, from normal transmission to propagation along a potential, allows graphene to be used as a switching device. The existence of bound modes within smooth potentials in graphene may provide an additional argument in favor of the mechanism for minimal conductivity, where charge puddles lead to a percolation network of conducting channels [74]. It can be seen from Eq. (21) that the exact solutions correspond to the case where there exists a bound state at equal energy above and below the top of the well. For example, a potential of characteristic strength  $w = 3.2$  with  $\Delta = 1.856$  contains seven bound modes, two of which are symmetric about  $E = 0$ , as shown in Fig. 4.

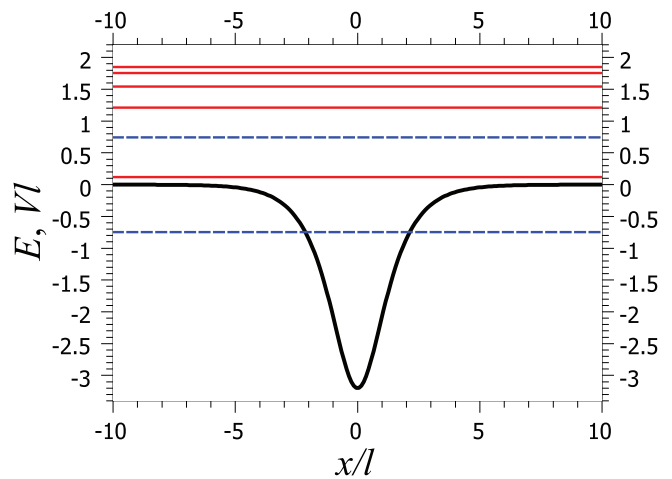


FIG. 4. (Color online) Schematic energy spectrum of  $-w/\cosh(x/l)$ , for the case of  $w = 3.2$  and  $\Delta = 1.856$ , in this instance there are seven eigenvalues. The solid (red) and long-dashed (blue) lines correspond to the calculated and exactly determined eigenvalues, respectively. The potential profile is shown in the same scale.

### III. CONCLUSIONS

We have presented quasi-exact solutions to the Dirac equation for the hyperbolic secant potential, which provides a good fit for potential profiles of existing top-gated graphene structures. It was found that bound states of both positive and negative energies exist in the energy spectrum and that there is a threshold value of  $w$ , the characteristic potential strength, for which the first mode appears.

### ACKNOWLEDGMENTS

We are grateful to Charles Downing for valuable discussions and thank Katrina Vargas and Elvis Arguelles for the critical reading of the manuscript. This work was supported by URCO (17 N 1TAY 12-1TAY 13), the EU FP7 ITN NOTEDEV (Grant No. FP7-607521), and FP7 IRSES projects SPINMET (Grant No. FP7-246784), QOCaN (Grant No. FP7-316432), and InterNoM (Grant No. FP7-612624).

### APPENDIX

List of eigenvalues and their corresponding  $\Delta_{n,m}$ :

$$\begin{aligned}
 E_{0,0} &= 0 \\
 E_{1,0} &= -\frac{1}{2w}\sqrt{w^2 - w} \\
 E_{1,1} &= -E_{1,0} \\
 E_{2,0} &= -\frac{1}{2w}\sqrt{4w^2 - 6w + 1} \\
 E_{2,1} &= 0 \\
 E_{2,2} &= -E_{2,0} \\
 E_{3,0} &= -\frac{1}{2w}\sqrt{5w^2 - 10w + 3 + \sqrt{16w^4 - 64w^3 + 85w^2 - 42w + 9}} \\
 E_{3,1} &= -\frac{1}{2w}\sqrt{5w^2 - 10w + 3 - \sqrt{16w^4 - 64w^3 + 85w^2 - 42w + 9}} \\
 E_{3,2} &= -E_{3,1} \\
 E_{3,3} &= -E_{3,0} \\
 E_{4,0} &= -\frac{1}{4w}\sqrt{40w^2 - 100w + 42 + 6\sqrt{16w^4 - 80w^3 + 140w^2 - 100w + 33}} \\
 E_{4,1} &= -\frac{1}{4w}\sqrt{40w^2 - 100w + 42 - 6\sqrt{16w^4 - 80w^3 + 140w^2 - 100w + 33}} \\
 E_{4,2} &= 0 \\
 E_{4,3} &= -E_{4,1} \\
 E_{4,4} &= -E_{4,0} \\
 \Delta_{0,0} &= \pm\left(w - \frac{1}{2}\right) \\
 \Delta_{1,0} = \Delta_{1,1} &= \pm\frac{1}{w}\sqrt{w^2 - w}\left(w - \frac{1}{2}\right) \\
 \Delta_{2,1} &= \pm\left(w - \frac{3}{2}\right) \\
 \Delta_{2,0} = \Delta_{2,2} &= \pm\frac{1}{2w}(2w^2 - 3w + 1) \\
 \Delta_{3,0} = \Delta_{3,3} &= \pm\frac{1}{2w}\sqrt{4w^4 - 16w^3 + 21w^2 - 10w + 3 + \sqrt{16w^4 - 64w^3 + 85w^2 - 42w + 9}} \\
 \Delta_{3,1} = \Delta_{3,2} &= \pm\frac{1}{2w}\sqrt{4w^4 - 16w^3 + 21w^2 - 10w + 3 - \sqrt{16w^4 - 64w^3 + 85w^2 - 42w + 9}} \\
 \Delta_{4,2} &= \pm\left(w - \frac{5}{2}\right) \\
 \Delta_{4,0} = \Delta_{4,4} &= \pm\frac{1}{2w}\left(\frac{3}{2} + \frac{1}{2}\sqrt{16w^4 - 80w^3 + 140w^2 - 100w + 33}\right) \\
 \Delta_{4,1} = \Delta_{4,3} &= \pm\frac{1}{2w}\left(\frac{3}{2} - \frac{1}{2}\sqrt{16w^4 - 80w^3 + 140w^2 - 100w + 33}\right)
 \end{aligned}$$

[1] N. Dombey, P. Kennedy, and A. Calogeracos, *Phys. Rev. Lett.* **85**, 1787 (2000).

[2] B. L. Coulter and C. G. Adler, *Am. J. Phys.* **39**, 305 (1971).

[3] A. Calogeracos, N. Dombey, and K. Imagawa, *Yad. Fiz.* **59**, 1331 (1996) [*Phys. At. Nucl.* **59**, 1275 (1996)].

[4] P. Kennedy, *J. Phys. A* **35**, 689 (2002).



- [5] V. M. Villalba and W. Greiner, *Phys. Rev. A* **67**, 052707 (2003).
- [6] J. Y. Guo, Y. Yu, and S. W. Jin, *Cent. Eur. J. Phys.* **7**, 168 (2009).
- [7] K. Sogut and A. Havare, *Phys. Scr.* **82**, 045013 (2010).
- [8] A. Arda, O. Aydogdu, and R. Sever, *Phys. Scr.* **84**, 025004 (2011).
- [9] V. M. Villalba and L. A. Gonzalez-Arraga, *Phys. Scr.* **81**, 025010 (2010).
- [10] P. Kennedy, N. Dombey, and R. L. Hall, *Int. J. Mod. Phys. A* **19**, 3557 (2004).
- [11] K. S. Novoselov, A. K. Geim, S. V. Morozov, D. Jiang, Y. Zhang, S. V. Dubonos, I. V. Grigorieva, and A. A. Firsov, *Science* **306**, 666 (2004).
- [12] A. H. Castro Neto, F. Guinea, N. M. R. Peres, K. S. Novoselov, and A. K. Geim, *Rev. Mod. Phys.* **81**, 109 (2007).
- [13] O. Klein, *Z. Phys.* **53**, 157 (1929).
- [14] T. Ando, T. Nakanishi, and R. Saito, *J. Phys. Soc. Jpn.* **67**, 2857 (1998).
- [15] M. I. Katsnelson, K. S. Novoselov, and A. K. Geim, *Nat. Phys.* **2**, 620 (2006).
- [16] T. Ya. Tudorovskiy and A. V. Chaplik, *JETP Lett.* **84**, 619 (2006).
- [17] J. M. Pereira, Jr., V. Mlinar, F. M. Peeters, and P. Vasilopoulos, *Phys. Rev. B* **74**, 045424 (2006).
- [18] H. C. Nguyen, M. T. Hoang, and V. L. Nguyen, *Phys. Rev. B* **79**, 035411 (2009).
- [19] F. M. Zhang, Y. He, and X. Chen, *Appl. Phys. Lett.* **94**, 212105 (2009).
- [20] J. H. Bardarson, M. Titov, and P. W. Brouwer, *Phys. Rev. Lett.* **102**, 226803 (2009).
- [21] J. R. Williams, T. Low, M. S. Lundstrom, and C. M. Marcus, *Nat. Nanotechnol.* **6**, 222 (2011).
- [22] J. H. Yuan, Z. Cheng, Q. J. Zeng, J. P. Zhang, and J. J. Zhang, *J. Appl. Phys.* **110**, 103706 (2011).
- [23] Z. H. Wu, *Appl. Phys. Lett.* **98**, 082117 (2011).
- [24] C. A. Downing, D. A. Stone, and M. E. Portnoi, *Phys. Rev. B* **84**, 155437 (2011).
- [25] P. Ping, Z. Peng, L. Jian-Ke, C. Zhen-Zhou, and L. Guan-Qiang, *Commun. Theor. Phys.* **58**, 765 (2012).
- [26] T. Tudorovskiy, K. J. A. Reijnders, and M. I. Katsnelson, *Phys. Scr. T* **146**, 014010 (2012).
- [27] D. S. Miserev and M. V. Entin, *Zh. Eksp. Teor. Fiz.* **142**, 784 (2012) [*JETP* **115**, 694 (2012)].
- [28] K. J. A. Reijnders, T. Tudorovskiy, and M. I. Katsnelson, *Ann. Phys.* **333**, 155 (2013).
- [29] J. M. Pereira, F. M. Peeters, and P. Vasilopoulos, *Phys. Rev. B* **75**, 125433 (2007).
- [30] A. De Martino, L. Dell'Anna, and R. Egger, *Phys. Rev. Lett.* **98**, 066802 (2007).
- [31] A. De Martino, *Solid State Commun.* **144**, 547 (2007).
- [32] A. V. Shytov, M. S. Rudner, and L. S. Levitov, *Phys. Rev. Lett.* **101**, 156804 (2008).
- [33] L. Dell'Anna and A. De Martino, *Phys. Rev. B* **79**, 045420 (2009).
- [34] S. Ghosh and M. Sharma, *J. Phys.: Condens. Matter* **21**, 292204 (2009).
- [35] T. K. Ghosh, *J. Phys.: Condens. Matter* **21**, 045505 (2009).
- [36] S. Kuru, J. M. Negro, and L. M. Nieto, *J. Phys.: Condens. Matter* **21**, 455305 (2009).
- [37] M. Sharma and S. Ghosh, *J. Phys.: Condens. Matter* **23**, 055501 (2011).
- [38] N. Myoung, G. Ihm, and S. J. Lee, *Phys. Rev. B* **83**, 113407 (2011).
- [39] W. D. Huang, Y. He, Y. F. Yang, and C. F. Li, *J. Appl. Phys.* **111**, 053712 (2012).
- [40] T. Low and F. Guinea, *Nano. Lett.* **8**, 2442 (2008).
- [41] V. M. Pereira and A. H. Castro Neto, *Phys. Rev. Lett.* **103**, 046801 (2009).
- [42] F. Guinea, M. I. Katsnelson, and A. K. Geim, *Nat. Phys.* **6**, 30 (2010).
- [43] Z. H. Wu, F. Zhai, F. M. Peeters, H. Q. Xu, and K. Chang, *Phys. Rev. Lett.* **106**, 176802 (2011).
- [44] V. V. Cheianov and V. I. Fal'ko, *Phys. Rev. B* **74**, 041403(R) (2006).
- [45] J. M. Pereira, Jr., P. Vasilopoulos, and F. M. Peeters, *Appl. Phys. Lett.* **90**, 132122 (2007).
- [46] C. W. J. Beenakker, *Rev. Mod. Phys.* **80**, 1337 (2008).
- [47] M. M. Fogler, D. S. Novikov, L. I. Glazman, and B. I. Shklovskii, *Phys. Rev. B* **77**, 075420 (2008).
- [48] L. M. Zhang and M. M. Fogler, *Phys. Rev. Lett.* **100**, 116804 (2008).
- [49] J. R. Williams, L. DiCarlo, and C. M. Marcus, *Science* **317**, 638 (2007).
- [50] B. Huard, J. A. Sulpizio, N. Stander, K. Todd, B. Yang, and D. Goldhaber-Gordon, *Phys. Rev. Lett.* **98**, 236803 (2007).
- [51] B. Özyilmaz, P. Jarillo-Herrero, D. Efetov, D. A. Abanin, L. S. Levitov, and P. Kim, *Phys. Rev. Lett.* **99**, 166804 (2007).
- [52] R. V. Gorbachev, A. S. Mayorov, A. K. Savchenko, D. W. Horsell, and F. Guinea, *Nano Lett.* **8**, 1995 (2008).
- [53] G. Liu, J. Velasco, Jr., W. Bao, and C. N. Lau, *Appl. Phys. Lett.* **92**, 203103 (2008).
- [54] N. Stander, B. Huard, and D. Goldhaber-Gordon, *Phys. Rev. Lett.* **102**, 026807 (2009).
- [55] A. F. Young and P. Kim, *Nat. Phys.* **5**, 222 (2009).
- [56] A. El Mouhafid and A. Jellal, *J. Low Temp. Phys.* **173**, 264 (2013).
- [57] R. R. Hartmann, N. J. Robinson, and M. E. Portnoi, *Phys. Rev. B* **81**, 245431 (2010).
- [58] D. A. Stone, C. A. Downing, and M. E. Portnoi, *Phys. Rev. B* **86**, 075464 (2012).
- [59] P. R. Wallace, *Phys. Rev.* **71**, 622 (1947).
- [60] D. Dragoman, *Phys. Scr.* **79**, 15003 (2009).
- [61] A. V. Turbiner, *Sov. Phys. JETP* **67**, 230 (1988); *Commun. Math. Phys.* **118**, 467 (1988).
- [62] A. G. Ushveridze, *Quasi-exactly Solvable Models in Quantum Mechanics* (Taylor and Francis, New York, 1994).
- [63] C. M. Bender and S. Boettcher, *J. Phys. A* **31**, L273 (1998).
- [64] C. A. Downing, *J. Math. Phys.* **54**, 072101 (2013).
- [65] R. R. Hartmann, I. A. Shelykh, and M. E. Portnoi, *Phys. Rev. B* **84**, 035437 (2011).
- [66] B. Sutherland and D. C. Mattis, *Phys. Rev. A* **24**, 1194 (1981).
- [67] M. G. Calkin, D. Kiang, and Y. Nogami, *Am. J. Phys.* **55**, 737 (1987).
- [68] B. H. J. McKellar and G. J. Stephenson, Jr., *Phys. Rev. C* **35**, 2262 (1987).
- [69] F. A. B. Coutinho, Y. Nogami, and F. M. Toyama, *Rev. Bras. Ensino Fís.* **31**, 4302 (2009).
- [70] K. Heun, *Math. Ann.* **33**, 161 (1889).
- [71] M. Hortaçsu, arXiv:1101.0471.
- [72] R. S. Maier, *Math. Comp.* **76**, 811 (2007).
- [73] R. S. Maier, *J. Differ. Equations* **213**, 171 (2005).
- [74] V. V. Cheianov, V. I. Fal'ko, B. L. Altshuler, and I. L. Aleiner, *Phys. Rev. Lett.* **99**, 176801 (2007).